Prognostic Value of O-(2-^{18}F-Fluoroethyl)-L-Tyrosine PET and MRI in Low-Grade Glioma

Frank W. Floeth[1], Dirk Pauleit[2,3], Michael Sabel[1], Gabriele Stoffels[2,3], Guido Reifenberger[4], Markus J. Riemenschneider[4], Paul Jansen[5], Heinz H. Coenen[3,6], Hans-Jakob Steiger[1], and Karl-Josef Langen[2,3]

[1]Department of Neurosurgery, Heinrich-Heine-University, Düsseldorf, Germany; [2]Institute of Medicine, Research Center Jülich, Jülich, Germany; [3]Brain Imaging Center West, Research Center Jülich, Jülich, Germany; [4]Department of Neuropathology, Heinrich-Heine-University, Düsseldorf, Germany; [5]Central Institute of Applied Mathematics, Research Center Jülich, Jülich, Germany; and [6]Institute of Nuclear Chemistry, Research Center Jülich, Jülich, Germany

In glioma of World Health Organization (WHO) grade II (low-grade glioma), the natural course of a particular patient is not predictable and the treatment strategy is controversial. We determined prognostic factors in adult patients with untreated, nonenhancing, supratentorial low-grade glioma with special regard to PET using the amino acid O-(2-^{18}F-fluoroethyl)-L-tyrosine (^{18}F-FET) and MRI. **Methods:** In a prospective study, baseline ^{18}F-FET PET and MRI analyses were performed on 33 consecutive patients with histologically confirmed low-grade glioma. None of the patients had radiation or chemotherapy. Clinical, histologic, therapeutic (initial cytoreduction vs. biopsy), ^{18}F-FET uptake, and MRI morphologic parameters were analyzed for their prognostic significance. Statistical endpoints were clinical or radiologic tumor progression, malignant transformation to glioma of WHO grade III or IV (high-grade glioma), and death. **Results:** Baseline ^{18}F-FET uptake and a diffuse versus circumscribed tumor pattern on MRI were highly significant predictors of prognosis ($P < 0.01$). By the combination of these prognostically significant variables, 3 major prognostic subgroups of low-grade glioma patients could be identified. The first of these subgroups was patients with circumscribed low-grade glioma on MRI without ^{18}F-FET uptake ($n = 11$ patients, progression in 18%, no malignant transformation and no death). The second subgroup was patients with circumscribed low-grade glioma with ^{18}F-FET uptake ($n = 13$ patients, progression in 46%, malignant transformation to a high-grade glioma in 15%, and death in 8%). The third subgroup was patients with diffuse low-grade glioma with ^{18}F-FET uptake ($n = 9$ patients, progression in 100%, malignant transformation to a high-grade glioma in 78%, and death in 56%). **Conclusion:** We conclude that baseline amino acid uptake on ^{18}F-FET PET and a diffuse versus circumscribed tumor pattern on MRI are strong predictors for the outcome of patients with low-grade glioma.

Key Words: low-grade glioma; prognosis; amino acid PET; O-(2-^{18}F-fluoroethyl)-L-tyrosine (^{18}F-FET); circumscribed lesion; diffuse lesion

Gliomas of WHO grade II (low-grade gliomas) account for approximately 15% of all astrocytic and oligodendroglial gliomas (*1*). Although some patients with low-grade glioma have stable disease and an excellent quality of life for decades without therapy, others experience rapid tumor progression and a poor prognosis. Epidemiologic data indicate that longer survival is associated with factors such as younger age, histologic type, and surgical treatment (*2*). The radical resection of low-grade glioma in noneloquent areas has proven to increase life expectancy (*3–8*). In small tumors, up to a diameter of 3 cm, interstitial radiosurgery (brachytherapy with radioactive seeds) reaches results that are comparable to those of radical tumor resection (*9*).

Moreover, the presence of chronic epilepsy in the absence of focal neurologic deficits has been described as a factor associated with favorable outcome (*3*). Risk factors for an unfavorable outcome include a tumor volume of more than 20 mL with a consecutive mass shift, contrast enhancement on MRI, and a gemistocytic astrocytic histologic type (*9,10*).

Nevertheless, the natural course of disease is not yet predictable in individual patients, and the treatment strategy remains controversial (*11,12*). A better stratification between patients with clinically indolent tumors and patients with aggressive tumors would be of paramount importance for optimal treatment.

Metabolic imaging using PET and ^{18}F-FDG is helpful for identifying malignant transformation in cerebral gliomas; however, ^{18}F-FDG uptake is generally low in low-grade glioma (*13*). In contrast, uptake of radiolabeled amino acids is increased in approximately two thirds of low-grade glioma, and a prognostic role for amino acid PET in low-grade glioma has been proposed (*14,15*). O-(2-^{18}F-Fluoroethyl)-L-tyrosine (^{18}F-FET) is a new PET tracer that—in contrast to other amino acid tracers—fulfills all requirements for routine clinical application, similar to the widely used ^{18}F-FDG (*16*). In this prospective study, we evaluated the prognostic role of MRI and [8]F-FET PET in adults with untreated supratentorial low-grade glioma.

MATERIALS AND METHODS

Patient Population

Within the 7-y period of 1999–2005, a group of 33 consecutive patients with low-grade glioma were included in the study. All had newly diagnosed, previously untreated supratentorial low-grade glioma without signs of blood–brain barrier disruption on contrast-enhanced MRI. Patients with infratentorial, thalamic, and hypothalamic tumors; children; and patients with low-grade glioma with contrast enhancement on MRI were excluded because of their different biologic and prognostic behavior. All patients were eligible for elective treatment planning—that is, were in stable clinical and neurologic condition without signs or symptoms of increased intracranial pressure. Detailed information on the individual patients is given in Tables 1 and 2. The study was approved by the university ethics committee and federal authorities. All subjects gave written informed consent for their participation in the study.

TABLE 1
Prognostic Variables

Patient no.	Sex	Age* (y)	MRI features† Side	Location	Shift	Diffuse	FET uptake‡ Mean	>1.1	Max	Initial therapy	Initial cytoreduction§	Initial histology‖	Mib1¶	p53#
Group A														
1	M	32	L	O	−	−	0.7	−	1.2	Resection	Total	A II	2	3
2	M	48	L	P	−	−	0.8	−	1.2	Biopsy	−	A II	1	2
3	M	47	L	F	−	−	0.8	−	1.1	Biopsy	−	A II	1	1
4	M	48	L	F (-T)	+	−	0.9	−	1.5	Biopsy	−	A II	1	2
5	F	41	R	F	−	−	0.9	−	1.2	Biopsy	−	A II	1	3
6	F	45	R	F	+	−	0.9	−	1.7	Resection	Total	A II	1	3
7	F	40	L	F	+	−	0.9	−	2.1	Resection	Subtotal	A II	1	3
8	M	42	R	F	+	−	1.0	−	1.9	Resection	Partial	A II	2	3
9	M	44	L	F (-T)	+	−	1.0	−	1.8	Biopsy	−	A II	1	2
10	M	35	L	T (-O)	−	−	1.1	−	1.4	Biopsy	−	A II	2	2
11	F	45	R	P	−	−	1.1	−	1.7	Biopsy	−	A II	1	3
Group B														
12	M	35	L	F (-T)	+	−	1.2	+	1.8	Biopsy	−	A II	1	0
13	M	40	L	T (-O)	−	−	1.4	+	1.5	Biopsy	−	A II	1	1
14	F	37	L	F (-T)	−	−	1.6	+	2.4	Resection	Subtotal	OA II	1	0
15	M	27	L	T	−	−	1.6	+	2.0	Biopsy	−	A II	1	3
16	M	47	L	P	−	−	1.7	+	2.0	Resection	Subtotal	OA II	1	0
17	F	53	L	P	−	−	1.7	+	2.3	Biopsy	−	A II	1	0
18	M	37	L	F	−	−	1.8	+	2.7	Resection	Subtotal	A II	1	0
19	M	32	R	P	−	−	2.0	+	2.7	Resection	Partial	A II	1	0
20	F	36	R	F	−	−	2.0	+	2.8	Resection	Total	O II	1	0
21	M	34	R	T (-O)	−	−	2.1	+	3.0	Biopsy	−	O II	1	0
22	M	32	L	T	−	−	2.2	+	4.7	Biopsy	−	A II	2	2
23	M	29	R	T (-O)	+	−	2.3	+	4.1	Biopsy	−	A II	2	1
24	F	53	L	F (-T)	+	−	2.8	+	5.1	Biopsy	−	A II	1	2
Group C														
25	M	61	R	F (-P)	−	+	1.3	+	1.6	Biopsy	−	O II	1	0
26	M	39	R	F	−	+	1.6	+	2.0	Biopsy	−	A II	1	4
27	F	41	L	P	+	+	1.6	+	2.3	Biopsy	−	O II	1	0
28	F	34	L	T (-O)	+	+	1.7	+	1.7	Resection	Partial	A II	1	3
29	F	44	L	F	−	+	1.9	+	2.8	Biopsy	−	A II	0	0
30	F	33	L	F	+	+	1.9	+	1.9	Biopsy	−	A II	1	4
31	M	43	R	F (-T)	+	+	1.9	+	1.9	Resection	Subtotal	A II	1	2
32	M	31	R	P	−	+	2.3	+	4.6	Resection	Subtotal	A II	2	3
33	F	65	L	F	+	+	2.4	+	3.9	Biopsy	−	A II	1	3

*At initial diagnosis.

†L = left hemisphere; R = right hemisphere; O = occipital; P = parietal; F = frontal; T = temporal. In "shift" category, + = space-occupying lesion with ventricular compression or midline shift; in "diffuse" category, + = diffuse lesion (ill-defined borders with inhomogeneous MRI signal), and − = circumscribed lesion (well-defined borders with homogeneous MRI signal).

‡Mean = tumor-to-brain ratio for entire MRI-defined lesion; max = maximum ratio for hot spots within lesion; + = mean ratio above 1.1 threshold; − = mean ratio at or below 1.1 threshold.

§Tumor mass resection > 90% (total), 50%–90% (subtotal), or < 50% (partial).

‖A II = astrocytoma WHO grade II; OA II = oligoastrocytoma WHO grade II; O II = oligodendroglioma WHO grade II.

¶On Ki67 labeling: 0 = no Mib1-positive cells; 1 = less than 1% Mib1-positive cells; 2 = between 1% and <5% Mib1-positive cells.

#0 = no p53-positive cells; 1 = individual p53-positive cells; 2 = moderate fraction of p53-positive cells; 3 = high fraction of p53-positive cells; 4 = not determined.

TABLE 2
Course and Outcome

Patient no.	Tumor progression during follow-up			Second therapy[†]	Malignant transformation[‡]	Second histology[§]	Death	Survival (mo)	
	Diagnosed	Clinically evident	Radiologically evident*					Progression-free	Overall[‖]
Group A									
1	+	−	Enlargement	Res	−	A II	−	31	33
2	−	−	−	−	−		−	67	67
3	+	−	Enhancement	Res	−	A II	−	60	65
4	−	−	−	−	−		−	48	48
5	−	−	−	−	−		−	46	46
6	−	−	−	−	−		−	10	10
7	−	−	−	−	−		−	7	7
8	−	−	−	−	−		−	26	26
9	−	−	−	−	−		−	8	8
10	−	−	−	−	−		−	36	36
11	−	−	−	−	−		−	10	10
Group B									
12	+	+	Enlargement	Res	−	A II	−	25	39
13	+	−	Enlargement	Res	−	A II	−	12	19
14	−	−	−	−	−		−	18	18
15	−	−	−	−	−		−	10	10
16	−	−	−	−	−		−	8	8
17	+	−	Enlargement, enhancement	Res, rad, chem	+	A III	−	39	41
18	−	−	−	−	−		−	32	32
19	−	−	−	−	−		−	17	17
20	−	−	−	−	−		−	10	10
21	−	−	−	−	−		−	24	24
22	+	−	Enhancement	Res, rad, chem	+	OA III	−	38	64
23	+	+	Enlargement	Res, rad	−	A II	+	6	9
24	+	+	Enlargement	Res	−	A II	−	43	50
Group C									
25	+	+	Enlargement	Observation	−		+	2	10
26	+	+	Enlargement, enhancement	Res, rad, chem	+	GB IV	−	9	10
27	+	−	Enhancement	Res, rad, chem	+	OA III	+	27	39
28	+	+	Enlargement, enhancement	Res, rad, chem	+	A III	+	10	14
29	+	−	Enhancement	Res, rad, chem	+	OA III	−	14	44
30	+	−	Enlargement, enhancement	Res, rad, chem	+	A III	−	24	26
31	+	+	Enlargement, enhancement	Res, rad, chem	+	GB IV	+	17	38
32	+	−	Enhancement	Res, rad, chem	+	OA III	−	7	24
33	+	+	Enlargement	Observation	−		+	12	22

*Enlargement = significant tumor growth; enhancement = new area of contrast enhancement on MRI.

[†]After diagnosis of progression: res = tumor resection; rad = radiation; chem = chemotherapy.

[‡]+ = first progression with malignant transformation from low-grade to high-grade glioma; − = first progression with continuing histology of low-grade glioma.

[§]After resection of progressive or recurrent tumor: A II = astrocytoma WHO grade II; AA III = anaplastic astrocytoma WHO grade III; AOA III = anaplastic oligoastrocytoma WHO grade III; GB IV = glioblastoma WHO grade IV.

[‖]Within the follow-up period of the particular patient.

Thirteen of the patients were female and 20 were male; age at diagnosis ranged from 27 to 65 y, with a mean of 40.9 y. Karnofsky performance status ranged from 90% to 100%, with a mean of 93%. Initial symptoms were seizures in 28 patients (85%), unspecific symptoms in 3 patients (9%), and focal neurologic deficits in 2 patients (6%).

The histologic diagnosis of low-grade glioma was established in all patients on tissue samples obtained by neuronavigated biopsy as described previously (17,18). In short, PET images were coregistered with MR images using dedicated software (MPI tool 3.28; ATV) and transferred to the neuronavigation system (Vector Vision; BrainLab). For coregistration, anatomic landmarks and external cutaneous fiducial markers were used in each examination. Neuronavigated biopsy samples were taken of FET-positive lesions from the area with maximal FET uptake. For FET-negative lesions, biopsy samples were taken only from areas showing an abnormal MRI signal.

Diffuse astrocytoma was diagnosed in 27 patients (82%), oligodendroglioma in 4 (12%), and oligoastrocytoma in 2 (6%). Subsequent first-line cytoreductive surgery was recommended in all patients with space-occupying tumors causing a clinically significant mass shift or tumors in noneloquent areas. According to these criteria, open surgery was offered to 20 patients, but 8 patients refused. Thus, surgery was performed on the remaining 12 patients. In 3 patients, resection was classified as "total" ($>$90% of the tumor volume was resected); in 6 patients, "subtotal" (50%–90% of the tumor mass was resected); and in 3 patients, "partial" ($<$50% of the tumor mass was resected). None of the patients received radiotherapy or chemotherapy as first-line therapy after biopsy or resection. Clinical and MRI follow-up was performed at regular intervals of 3–4 mo. The endpoints of course and outcome were tumor progression, malignant transformation to a glioma of WHO grade III or IV (high-grade glioma), and death of the patient.

Tumor progression was defined as clinical or radiologic deterioration. Symptoms and signs of clinical deterioration included new onset or aggravation of preexisting focal deficits or new onset of symptoms of increased intracranial pressure. Increased seizure activity was not regarded as a symptom of tumor progression. Radiologic deterioration was defined as a new onset of contrast enhancement within the tumor, significant enlargement of more than 20% of the initial tumor volume, or an increasing mass shift.

MRI

MRI was performed on a 1.5-T system (Sonata; Siemens). The imaging protocol consisted of a T1-weighted 3-dimensional magnetization-prepared rapid-acquisition gradient-echo sequence (field of view, 25 cm; matrix, 205×256; repetition time, 2,200 ms; echo time, 3.9 ms; inversion time, 1,200 ms; flip angle, 15; number of slices, 128; slice thickness, 1.5 mm; slice gap, 0 mm; number of averages, 1; time of acquisition, 6:38 min) before and 2 min after injection of 20 mL of gadolinium-diethylenetriaminepentaacetic acid (Magnevist; Schering) and a transversal fluid-attenuation inversion-recovery (FLAIR) sequence (field of view, 25 cm; matrix, 205×256; repetition time, 9,000 ms; echo time, 119 ms; inversion time, 2,500 ms; flip angle, 90; number of slices, 25; slice thickness, 5 mm; slice gap, 0 mm; number of averages, 2; time of acquisition, 4:32 min).

MRI scans were assessed by a senior neuroradiologist and 2 experienced senior neurosurgeons and scored by consensus. None of the tumors showed significant contrast enhancement after injection of gadolinium-diethylenetriaminepentaacetic acid. The tumor size was difficult to measure reliably because volumetric assessment was possible only for circumscribed tumors with well-defined borders—not for diffuse lesions. For semiquantitative evaluation, tumor size was estimated by the maximal cross-sectional diameter of the hypointense area on the T1-weighted images with respect to the hyperintensity on the FLAIR sequence. Tumors with a diameter greater than 30 mm were classified as large. According to their appearance on MRI, the tumors were classified as circumscribed in 24 patients (73%) and diffuse in 9 patients (27%). Circumscribed tumors were characterized by a homogeneous structure and sharp borders that were identical on T1- and T2-weighted images. Diffuse tumors showed an inhomogeneous signal pattern and poorly defined borders on MRI. In these tumors, the extent of hyperintensity on T2-weighted sequences was generally larger than the area of hypointensity on T1-weighted, indicating perifocal edema. Displacement of the brain midline by more than 2 mm was classified as a mass shift.

18F-FET PET

The patients were examined by ^{18}F-FET PET within 6 wk after the initial diagnosis and no more than 3 wk before the neuronavigated biopsy. The amino acid ^{18}F-FET was produced via phase transfer–mediated nucleophilic ^{18}F-fluorination of N-trityl-O-(2-tosyloxyethyl)-L-tyrosine tert-butyl ester and subsequent deprotection (19). The uncorrected radiochemical yield was about 35% at a specific radioactivity of more than 200 GBq/μmol and a radiochemical purity of more than 98%. The tracer was administered as an isotonic neutral solution. PET studies were acquired 15–40 min after the intravenous injection of 200 MBq of ^{18}F-FET. The measurements were performed on an ECAT scanner with 32 rings and an axial field of view of 15.5 cm (EXACT HR+; Siemens Medical Systems), in 3-dimensional mode. For attenuation correction, transmission scans with three ^{68}Ge/^{68}Ga rotating line sources were measured. After correction for random and scattered coincidences and dead time, image data were obtained by filtered backprojection in Fourier space using the ECAT 7.2 software (direct inverse Fourier transformation; Shepp filtering [2.48 mm in full width at half maximum]; pixel size, $2 \times 2 \times 2.4$ mm). The reconstructed images were decay-corrected; the reconstructed image resolution was about 5.5 mm.

Preoperative MR images and ^{18}F-FET PET images were coregistered and evaluated using regions of interest (ROIs) and dedicated software (MPI tool, version 3.28; ATV). For tumors with increased ^{18}F-FET uptake, the transaxial slice showing the highest tumor intensity was chosen and an isocontour region around the tumor maximum was drawn automatically using a cutoff of 3 SDs above the average activity in the reference region. A larger reference ROI was placed on the contralateral hemisphere in an area of normal-appearing brain that included white and gray matter. Because one third of the low-grade glioma exhibited indifferent ^{18}F-FET uptake, an objective positioning of the ROI on the PET scan based on threshold values was impossible. Therefore, a single irregular ROI was placed manually in an area of signal abnormality on the T1- and T2-weighted transversal MRI scan and transferred to the coregistered ^{18}F-FET PET scan in each case. Mean and maximal lesion-to-brain ratios were calculated by dividing the mean and maximal ROI value (Bq/mL) of the lesion by the mean ROI value of normal brain in the ^{18}F-FET PET scan. In a previous biopsy-controlled study, we found for tissue samples corresponding to normal and peritumoral tissue a mean lesion-to-brain ratio of 1.2 ± 0.4 for ^{18}F-FET uptake (17,18). For prognostic purposes, however, a statistical preevaluation with different mean lesion-to-brain ratios identified a threshold value of 1.1 as optimal for predicting the course and outcome of the patients. Therefore, in this study, lesions with a mean lesion-to-brain ratio of 1.1 or less for tracer uptake were judged as ^{18}F-FET–negative and lesions with a ratio of more than 1.1 as ^{18}F-FET–positive. For the maximum lesion-to-brain ratios, a threshold value of 2.0 was chosen indicating hot-spot areas in the tumors.

Histopathology

Initial cytologic assessment was performed on touch preparations during biopsy to ensure representative tissue sampling for subsequent routine histologic preparations. The final diagnoses were established on formalin-fixed and paraffin-embedded tissue samples according to the WHO classification of tumors of the nervous system (20). Additional immunohistochemical analyses were performed with antibodies against the tumor suppressor protein p53 (Clone D07, primary antibody dilution: 1:100; Dako) and the

proliferation-associated antigen Ki-67 (Clone Mib1, primary antibody dilution: 1:200; Dako) according to standard protocols. Immunohistochemical results were quantified using the following semiquantitative staining scores: for Ki-67, 0 (no positive tumor cells), 1 ($<$1% positive tumor cells), 2 (1%–5% positive tumor cells), or 3 ($>$5% positive tumor cells) and for p53, 0 (no positive tumor cells), 1 (individual positive tumor cells), 2 (moderate fraction of positive tumor cells [$<$50%]), or 3 (high fraction of positive tumor cells [$\geq$50%]).

Statistical Analysis

The prognostic significance of various factors regarding the primary endpoints was determined using the Kaplan–Meier method and tested using censored linear rank tests, with each factor considered a separate, independent variable. The computations were done with the LIFETEST procedure of SAS system release 9.1 (SAS Institute Inc.). Probability values of less than 0.01 were considered significant. No correction for multiple statistical comparisons was done.

Two prognostically significant variables were identified that allowed for the definition of 3 prognostic groups. The homogeneity of the distributions of each of 3 variables—"time until progression," "time until malignant transformation," and "time until death"—over these groups was tested using the log-rank test. The rank tests for the association of these 3 variables with each of the other factors (Table 3) adjusted for group levels were not significant. Thereby, we excluded the possibility that the differences in clinical course and outcome between the 3 prognostic groups were influenced by a combination of other factors.

RESULTS

Prognostic Factors

An overview of the distribution of the clinical MRI, morphologic, PET metabolic, histologic, and therapeutic variables and the data on the patients' clinical courses and outcomes is given in Tables 1 and 2. The results of the statistical analysis are given in Table 3. A significant influence on the course of the disease was found for 2 prognostic variables only. The first of these—circumscribed versus diffuse tumor growth on baseline MRI—reached the highest level of significance, with P values of less than 0.0001 for time until progression, less than 0.0001 for time until malignant transformation, and 0.008 for time until death. The second of the significant variables was mean ^{18}F-FET uptake on baseline PET, with P values of 0.001 for time until progression and 0.006 for time until malignant transformation. Statistical significance was not reached for time until death ($P = 0.06$), but it is important to note that all 6 deaths occurred in patients with ^{18}F-FET–positive tumors.

Prognostic Groups

Through the combination of the 2 significant prognostic variables, 3 major prognostic groups were identified: patients having circumscribed tumors without ^{18}F-FET uptake (Fig. 1), patients having circumscribed tumors with ^{18}F-FET uptake, and patients having diffuse tumors with ^{18}F-FET uptake (Fig. 1). None of the patients had a diffuse

TABLE 3
P Values from Univariate Analysis with Log-Rank Tests for Determining Prognostic Significance of Variables Regarding the 3 Follow-up Endpoints

| Variable	Clinical/radiologic tumor progression	Malignant transformation from low- to high-grade glioma	Death due to Disease
Biologic variables			
Sex	0.70	0.34	0.69
Age	0.22	0.20	0.28
Age ($<$40 y/$\geq$40 y)	0.71	0.17	0.95
Seizure history (yes/no)	0.88	0.67	0.013
MRI features			
Hemispheric (right/left)	0.87	0.49	0.55
Brain lobe location	0.52	0.61	0.76
Deep/superficial	0.27	0.95	0.06
Circumscribed/diffuse	$<$0.0001	$<$0.0001	0.008
Size ($<$3 cm/$\geq$3 cm)	0.09	0.22	0.44
Mass shift (yes/no)	0.12	0.25	0.04
FET uptake			
Mean FET uptake	0.05	0.11	0.10
Mean FET uptake ($\leq$1.1/$>$1.1)	0.001	0.006	0.06
Maximum FET uptake	0.19	0.43	0.46
Maximum FET uptake ($\leq$2.0/$>$2.0)	0.50	0.42	0.83
Histologic features			
Astrocytoma/oligodendroglioma	0.89	0.96	0.35
Gemistocytic (yes/no)	0.81	0.20	0.58
Mib1	0.48	0.71	0.96
p53	0.49	0.69	0.75
Initial therapy			
Cytoreduction/biopsy	0.46	0.78	0.90
Resection (total/subtotal/partial)	0.79	0.82	0.84
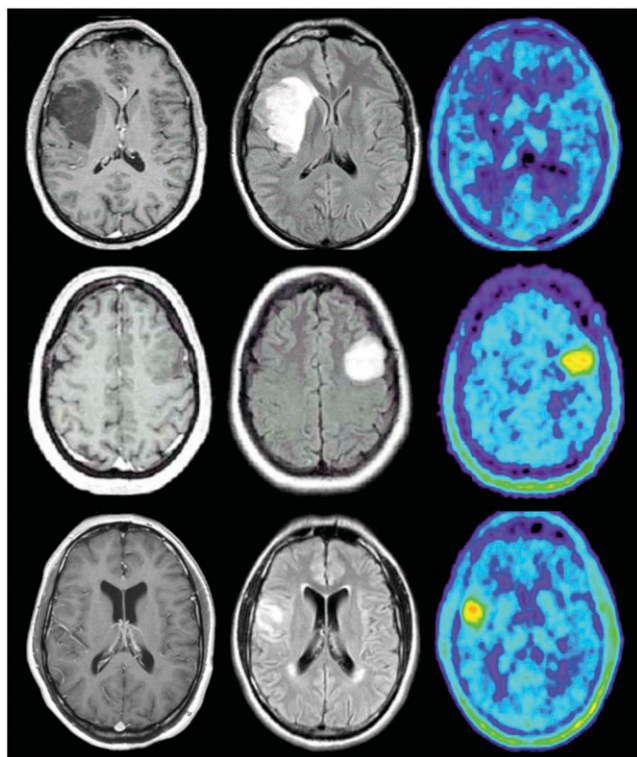
FIGURE 1. Examples of low-grade gliomas in prognostic groups A, B, and C. On the left are contrast-enhanced T1-weighted MR images, in the middle are T2-weighted MR images (FLAIR sequence), and on the right are ^{18}F-FET PET images. Top row (prognostic group A) shows circumscribed tumors and no FET uptake, middle row (prognostic group B) shows circumscribed tumors with increased FET uptake, and bottom row (prognostic group C) shows diffuse tumors with increased ^{18}F-FET uptake. Histopathology after biopsy showed diffuse astrocytoma of WHO grade II in each patient. None of the tumors showed contrast enhancement on T1-weighted MRI.

tumor without ^{18}F-FET uptake, thus excluding the creation of a fourth subgroup. Among the first, second, and third prognostic group, the number of patients (11, 13, and 9, respectively) and the average time of follow-up per patient (32, 26, and 29 mo, respectively) were fairly similar.

Statistical comparison of the 3 groups revealed significant differences in time until progression ($P < 0.0001$), time until malignant transformation ($P < 0.0001$), and time until death ($P = 0.01$) (Fig. 2). The rank tests for the association with each other factor proved that the differences between the 3 groups were not influenced by a combination of other factors. Figure 3 shows the Kaplan–Meier curves for time until progression in the 3 prognostic groups.

DISCUSSION

The clinical course and outcome of patients with supratentorial low-grade glioma may be highly variable. Several factors have been identified that are helpful for risk stratification, but a better identification of individuals with either a poor or a favorable prognosis is highly desirable

to optimize treatment. Delayed or insufficient treatment of progressive lesions may shorten survival time, whereas too early aggressive treatment may cause unnecessary hospitalization and treatment-related morbidity.

Contrast enhancement on MRI is generally thought to indicate malignant transformation, although a considerable fraction of cases of WHO grade III glioma may lack enhancement (18,21). Because of the inability of conventional radiologic imaging to provide reliable prognostic information, several other imaging modalities are under evaluation for brain tumors.

PET using ^{18}F-FDG is useful for identifying malignant transformation in cerebral gliomas, but ^{18}F-FDG uptake in low-grade glioma is generally low and does not allow for further differentiation of these tumors (13). Radiolabeled amino acids, such as [^{11}C-methyl]-L-methionine (MET), exhibit a variable uptake pattern in low-grade glioma (22), and low ^{11}C-MET uptake before treatment was found to be an important prognostic factor in these tumors (14). Tumor resection was reported to be favorable in low-grade glioma exhibiting high ^{11}C-MET uptake only (14). However, prospective studies dealing with these issues have not yet been published.

Unfortunately, the use of ^{11}C-MET is restricted to few centers because of the short physical half-life of the ^{11}C-label (20 min). In contrast, the amino acid ^{18}F-FET fulfills all requirements for widespread clinical application, that is, efficient radiosynthesis, ^{18}F labeling with a 109-min half-life, in vivo stability, and ideal tracer kinetics for brain tumor imaging (16,19,23,24). Results with ^{18}F-FET PET in brain tumors are similar to those with ^{11}C-MET (24,25), and the diagnostic potential of ^{18}F-FET PET in brain tumors is well documented—for example, a superior delineation of human gliomas by ^{18}F-FET PET compared with MRI (17), a high specificity for the detection of gliomas and biopsy site planning (18), and a reliable distinction between tumor recurrence and benign posttherapeutic changes (26).

The aim of this prospective study was to investigate the prognostic role of baseline ^{18}F-FET uptake in newly diagnosed low-grade glioma in relation to other prognostic parameters. We found that approximately two thirds of patients with low-grade glioma exhibited an increased ^{18}F-FET uptake compared with that in normal brain tissue, whereas one third of patients showed ^{18}F-FET uptake equal to or even less than that in normal brain tissue, a finding similar to previously observed results with ^{11}C-MET (22). In a statistical preevaluation, we found no significant prognostic difference between low-grade glioma with high ^{18}F-FET uptake (mean tumor-to-brain ratio > 2.5), low-grade glioma with moderate uptake (mean tumor-to-brain ratio of 1.6–2.5), and low-grade glioma with low uptake (mean tumor-to-brain ratio < 1.5). Also, the maximum tumor-to-brain ratio (^{18}F-FET uptake within hot-spot areas of the tumor) at a threshold of 2.0, which has been shown to be useful in separating recurrent gliomas from unspecific posttherapeutic changes (26), showed no significant effect on patient course and outcome. The further evaluation of different
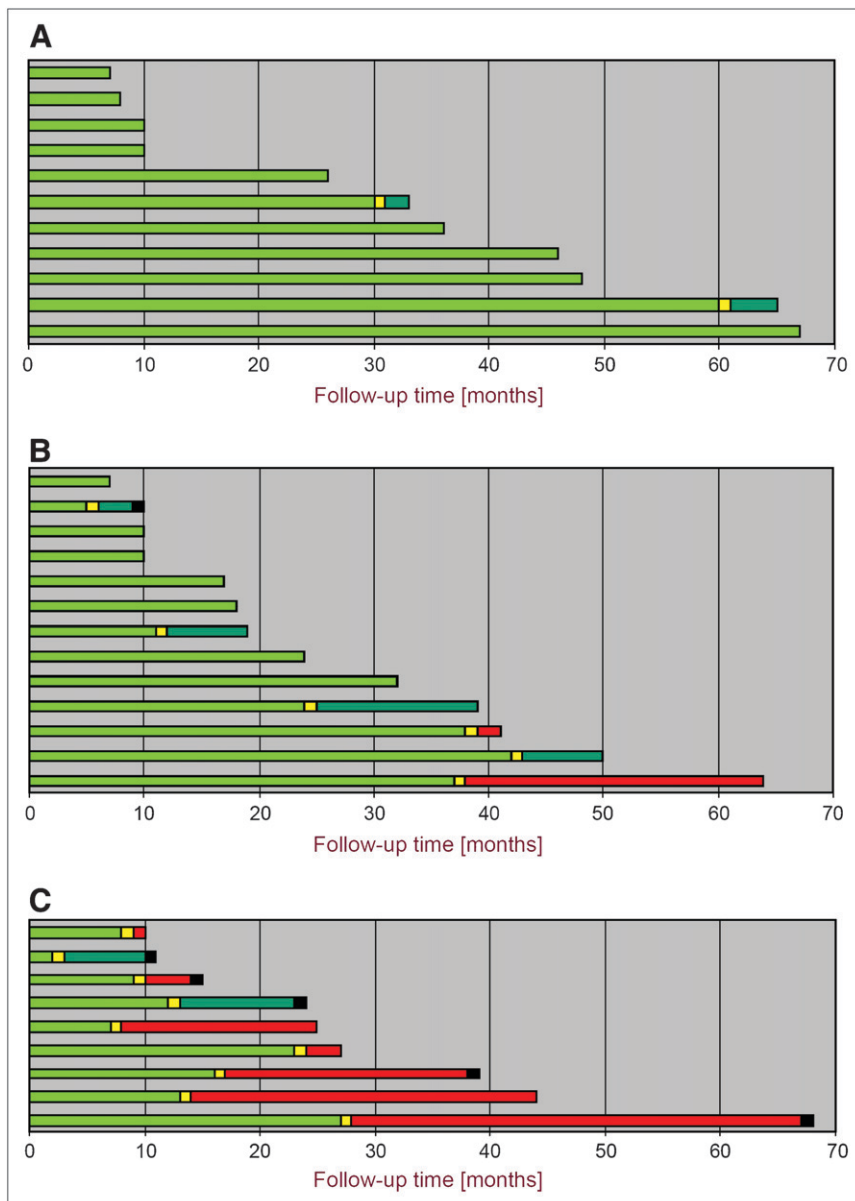
FIGURE 2. Graph of follow-up results for each patient. Green portion of each bar represents progression-free survival after initial diagnosis of low-grade glioma. Yellow portion indicates time of first tumor progression. If histology of low-grade glioma remained unchanged, color of bar stays green. If malignant transformation to high-grade glioma occurred, bar becomes red. Time of patient death is indicated by black portion of bar. (A) Prognostic group A, with favorable clinical course, rare progression of tumor (18%), and no malignant transformation or death during follow-up. (B) Prognostic group B, with less favorable clinical course, frequent tumor progression (46%), and sometimes early tumor progression. Small subsets of patients showed malignant transformation of tumors (15%) and/or died (8%) during follow-up. (C) Prognostic group C, with rapid clinical course and poor outcome, 100% tumor progression, and usually early tumor progression. Most patients showed malignant transformation of tumors (78%) and died of the disease (56%).

thresholds for low-grade glioma yielded significant prognostic differences in the mean tumor-to-brain ratio at thresholds of 1.1, 1.3, and 1.5, with a threshold of 1.1 providing the highest significance with regard to prognosis. It appears that the qualitative feature of increased ^{18}F-FET uptake itself is a more important prognostic factor than the degree of ^{18}F-FET uptake; that is, the most favorable prognosis for low-grade glioma is associated with an ^{18}F-FET uptake the same as or less than that of the surrounding brain tissue. Once a low-grade glioma exhibits increased ^{18}F-FET uptake, there seems to be a change in the biologic behavior, which is associated with a poor prognosis.

Somewhat unexpected was the observation that the MRI morphologic variable of a circumscribed versus diffuse tumor appearance had a highly significant influence on patient clinical course and outcome. Well-circumscribed

low-grade glioma (prognostic groups A and B in Fig. 1) can be considered the "typical" low-grade glioma, with a homogeneous and usually large lesion that can be diagnosed on MRI at first view. In contrast, diffuse low-grade glioma (prognostic group C in Fig. 1) represent a less typical low-grade glioma variant with an inhomogeneous, often small lesion that is difficult to assess because of the blurred tumor margins. The "diagnosis" of these tumors on the basis of the MRI scan is challenging.

Combination of 2 parameters—baseline ^{18}F-FET uptake at a threshold of 1.1 for mean tumor-to-brain ratio, and a diffuse versus circumscribed tumor pattern on MRI—revealed 3 major prognostic groups of patients (Fig. 1), and the statistical analysis proved that they had significant survival differences. Patients in prognostic group A, with circumscribed, ^{18}F-FET–negative low-grade glioma, generally showed a
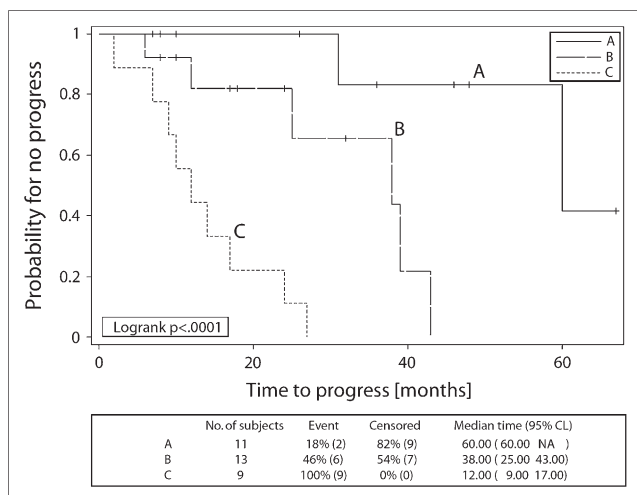
FIGURE 3. Example Kaplan–Meier plot of follow-up endpoint. Tumor progressed frequently (100%, $n = 9$) and early in prognostic group C, often (46%, $n = 6$) and sometimes early in prognostic group B, and rarely (18%, $n = 2$) and late in prognostic group A. Differences between the 3 groups were highly significant ($P < 0.0001$).

stable long-term clinical course and long survival without malignant transformation (Fig. 2A). Either total resection in cases of noneloquent tumor location, or otherwise biopsy and MRI follow-up, seems to be the appropriate therapy for these patients. Patients in prognostic group B had circumscribed, ^{18}F-FET–positive tumors. A fraction of these patients exhibited a poorer overall prognosis and early progression and malignant transformation to a high-grade glioma (Fig. 2B). Surgical resection should be attempted in these patients. Patients in prognostic group C had diffuse tumors with ^{18}F-FET uptake invariably associated with early progression, as well as frequent malignant transformation to high-grade glioma and death. Thus, cytoreductive surgery should always be attempted and adjuvant radiotherapy or chemotherapy should be considered in these patients. In addition, short follow-up intervals are warranted.

Except for these 2 survival factors, all other clinical and histologic variables tested in our study did not show a significant prognostic value, probably because of the relatively small number of patients. In contrast, the MRI- and ^{18}F-FET PET–based stratification of patients revealed clear prognostic differences, thus underlining the robustness and paramount clinical significance of this approach. Although MRI is widely available, the PET tracer ^{18}F-FET is not yet commonly on hand. ^{18}F-FET, however, fulfills all the requirements for becoming established on a widespread clinical scale within a short time.

Although tumor biopsy samples were taken using state-of-the-art methods, cell clones with a higher grade of malignancy might have been missed on the initial biopsy in some cases because of the limited tissue sampling. The proceedings in our study, however, reflect the situation under routine conditions, and the significance of our results for clinical practice is not affected. Especially, none of the WHO II

astrocytomas in group A showed malignant transformation within the period of observation.

A study period of 7 y represents a long time for a clinical investigation, but a follow-up of 10–15 y will be necessary to cover the average course of low-grade gliomas. Further patient follow-up is needed to evaluate overall survival data, and the recruitment of larger patient cohorts will help to generate additional data about the prognostic value of other potentially relevant parameters.

Recently, it was observed that a dynamic acquisition of ^{18}F-FET uptake may be helpful in differentiating between high-grade and low-grade gliomas (27,28). Although low-grade gliomas exhibited increasing lesion-to-brain ratios from 0 to 10 min after injection, compared with 30–40 min after injection, decreasing lesion-to-brain ratios were observed for high-grade gliomas. Dynamic data are not available for the present study but may be helpful in further studies to attain additional prognostic information from ^{18}F-FET PET data.

CONCLUSION

Our data indicate the existence of 2 strong predictors in determining the clinical course and outcome of adults with newly diagnosed, nonenhancing supratentorial low-grade glioma of WHO grade II: the morphologic feature of circumscribed versus diffuse tumor growth on baseline MRI, and the metabolic feature of the mean ^{18}F-FET uptake on baseline PET. The combination of these 2 variables defined 3 prognostically distinct groups of patients with low-grade glioma. Assignment of patients to these prognostic groups may allow for individually optimized and prognosis-related clinical management and therapy.

REFERENCES

1. Ohgaki H, Kleihues P. Population-based studies on incidence, survival rates, and genetic alterations in astrocytic and oligodendroglial gliomas. *J Neuropathol Exp Neurol.* 2005;64:479–489.
2. Claus EB, Black PM. Survival rates and patterns of care for patients diagnosed with supratentorial low-grade gliomas: data from the SEER program, 1973-2001. *Cancer.* 2006;106:1358–1363.
3. Piepmeier J, Christopher S, Spencer D, et al. Variations in the natural history and survival of patients with supratentorial low-grade astrocytomas. *Neurosurgery.* 1996;38:872–878.
4. Janny P, Cure H, Mohr M, et al. Low grade supratentorial astrocytomas: management and prognostic factors. *Cancer.* 1994;73:1937–1945.
5. Philippon JH, Clemenceau SH, Fauchon FH, Foncin JF. Supratentorial low-grade astrocytomas in adults. *Neurosurgery.* 1993;32:554–559.

6. Shaw EG, Daumas-Duport C, Scheihauer BW, et al. Radiation therapy in the management of low-grade supratentorial astrocytomas. *J Neurosurg.* 1989;70:853–861.

7. Laws ER Jr, Taylor WF, Clifton MB, Okazaki H. Neurosurgical management of low-grade astrocytoma of the cerebral hemispheres. *J Neurosurg.* 1984;61:665–673.

8. Keles GE, Lamborn KR, Berger MS. Low-grade hemispheric gliomas in adults: a critical review of extent of resection as a factor influencing outcome. *J Neurosurg.* 2001;95:735–745.

9. Kreth FW, Faist M, Warnke PC, et al. Interstitial radiosurgery of low-grade gliomas. *J Neurosurg.* 1995;82:418–429.

10. Kreth FW, Faist M, Rossner R, Volk B, Ostertag CB. Supratentorial World Health Organization Grade 2 astrocytomas and oligoastrocytomas: a new pattern of prognostic factors. *Cancer.* 1997;79:370–379.

11. Whittle IR. The dilemma of low grade glioma. *J Neurol Neurosurg Psychiatry.* 2004;75(suppl 2):31–36.

12. Wessels PH, Weber WE, Raven G, et al. Supratentorial grade II astrocytoma: biological features and clinical course. *Lancet Neurol.* 2003;2:395–403.

13. Chung JK, Kim YK, Kim SK, et al. Usefulness of ^{11}C-methionine PET in the evaluation of brain lesions that are hypo- or isometabolic on ^{18}F-FDG PET. *Eur J Nucl Med Mol Imaging.* 2002;29:176–182.

14. Ribom D, Eriksson A, Hartman M, et al. Positron emission tomography ^{11}C-methionine and survival in patients with low-grade gliomas. *Cancer.* 2001;92:1541–1549.

15. De Witte O, Goldberg I, Wikler D, et al. Positron emission tomography with injection of methionine as a prognostic factor in glioma. *J Neurosurg.* 2001;95:746–750.

16. Langen KJ, Hamacher K, Weckesser M, et al. O-(2-[^{18}F]fluoroethyl)-L-tyrosine: uptake mechanisms and clinical applications. *Nucl Med Biol.* 2006;33:287–294.

17. Pauleit D, Floeth F, Hamacher K, et al. O-(2-[^{18}F]fluoroethyl)-L-tyrosine PET combined with magnetic resonance imaging improves the diagnostic assessment of cerebral gliomas. *Brain.* 2005;128:678–687.

18. Floeth FW, Pauleit D, Wittsack HJ, et al. Multimodal metabolic imaging of cerebral gliomas: positron emission tomography with [^{18}F]fluoroethyl-L-tyrosine and magnetic resonance spectroscopy. *J Neurosurg.* 2005;102:318–327.

19. Hamacher K, Coenen HH. Efficient routine production of the ^{18}F-labelled amino acid O-(2-[^{18}F]fluoroethyl)-L-tyrosine. *Appl Radiat Isot.* 2002;57:853–856.

20. Kleihues P, Cavenee WK. *World Health Organization Classification of Tumours. Pathology and Genetics of Tumours of the Nervous System.* Lyon, France: IARC Press; 2000.

21. Scott JN, Brasher PM, Sevick RJ, Rewcastle NB, Forsyth PA. How often are nonenhancing supratentorial gliomas malignant? A population study. *Neurology.* 2002;59:947–949.

22. Herholz K, Holzer T, Bauer B, et al. ^{11}C-Methionine PET for differential diagnosis of low-grade gliomas. *Neurology.* 1998;50:1316–1322.

23. Wester HJ, Herz M, Weber W, et al. Synthesis and radiopharmacology of O-(2-[^{18}F]fluoroethyl)-L-tyrosine for tumor imaging. *J Nucl Med.* 1999;40:205–212.

24. Weber WA, Wester HJ, Grosu AL, et al. O-(2-[^{18}F]Fluoroethyl)-L-tyrosine and L-[methyl-^{11}C]methionine uptake in brain tumours: initial results of a comparative study. *Eur J Nucl Med.* 2000;27:542–549.

25. Langen KJ, Jarosch M, Muhlensiepen H, et al. Comparison of fluorotyrosines and methionine uptake in F98 rat gliomas. *Nucl Med Biol.* 2003;30:501–508.

26. Pöpperl G, Gotz C, Rachinger W, Gildehaus FJ, Tonn JC, Tatsch K. Value of O-(2-[^{18}F]fluoroethyl)-L-tyrosine PET for the diagnosis of recurrent glioma. *Eur J Nucl Med Mol Imaging.* 2004;31:1464–1470.

27. Weckesser M, Langen KJ, Rickert CH, et al. O-(2-[^{18}F]Fluorethyl)-L-tyrosine PET in the clinical evaluation of primary brain tumors. *Eur J Nucl Med Mol Imaging.* 2005;32:422–429.

28. Pöpperl G, Kreth FW, Herms J, et al. Analysis of ^{18}F-FET PET for grading of recurrent gliomas: is evaluation of uptake kinetics superior to standard methods? *J Nucl Med.* 2006;47:393–403.